

Abhinav Saxena, Nir Uriel, and Daniel Burkhoff

---

## Introduction

Left ventricular assist devices (LVADs) play a crucial role in providing hemodynamic support in patients with end-stage chronic heart failure. LVADs are used in patients awaiting cardiac transplantation by acting as a bridge to transplant (BTT) and as destination therapy (DT) in patients not eligible for heart transplant [1–3]. More recently, LVADs have been used as bridge to decision (BTD) in patients with uncertain eligibility for transplantation and as bridge to recovery (BTR) in critically ill patients expected to sufficiently or totally recover without the need for a transplant. Their use for all the above applications is expected to increase in the future as devices become more compact and safer to use.

LVADs actively interact with the native heart and circulation to effectively improve end-organ perfusion while unloading the left ventricle. These factors each contribute independently the

profound reverse ventricular remodeling observed during prolonged LVAD support [4]. Understanding the physiology of LVAD hemodynamics is vital for clinicians to improve patient care especially since there will be an increasing number of LVAD patients in the coming years. We therefore aim to present a clinically relevant review of the physiology of LVADs as applied to patients with chronic heart failure.

---

## Types of Ventricular Assist Device

The human heart is a complex volume displacement, pulsatile pump. First generation of LVAD's mimicked this concept. Due to their large size, high rates of adverse events, and device failures [5], their use was supplanted entirely as soon as smaller, continuous-flow devices became available.

Second-generation axial-flow pumps utilize a rotational pump design with ceramic contact bearings. The blood enters and is pushed forward by a screwing motion eventually exiting the pump coaxially [6]. Despite smaller size and higher long-term reliability due to only one moving part [7], contact bearings are prone to frictional wear overtime, incomplete bearing wash, potential for stasis, and thrombus formation at the rotor-bearing interface [8]. Further iterations resulted in the current third generation of pumps which are centrifugal in design with noncontact

---

A. Saxena, MBBS  
Maimonides Medical Center, Brooklyn, NY, USA

N. Uriel, MD  
Columbia and Cornell Universities, New York  
Presbyterian, New York, NY, USA  
e-mail: nu2126@cumc.columbia.edu

D. Burkhoff, MD, PhD (✉)  
Cardiovascular Research Foundation,  
New York, NY, USA  
e-mail: dburkhoff@crf.org



bearings. In these pumps, the blood enters the pump, is rotated by the impeller, and ejected at 90° to the inlet flow. The use of noncontact bearings facilitates increased blood flow around the impeller and better washing of the impeller surface. This is expected to increase pump longevity by reducing mechanical wear [9].

### Continuous-Flow Left Ventricular Assist Device (cf-LVAD) Hemodynamics

Cf-LVADs, including both axial and centrifugal pumps, impart kinetic energy and accelerate the blood by impeller rotation [10]. Pump function of cf-LVADs is characterized by pump speed (rpm), electrical power consumption (watts), flow (L/min), and the degree of pressure pulsatility during operation (via the pulsatility index, PI). The operator sets speed; power is a measure of current drawn by and voltage applied to the pump and relates for blood flow. In clinical practice, flow is not measured directly but is estimated from rotational speed (rpm) and power consumption in a majority of contemporary cf-LVADs; HeartAssist 5 and aVAD pumps use a transit-time ultrasonic probe to measure flow directly. The flow through the cf-LVADs is dictated by pump rotational speed, blood viscosity (related to hematocrit), preload pressure at the pump inlet, and afterload pressure at pump outlet according to the pump's unique pressure-flow characteristics, the HQ curve [11].

### Pressure-Flow Relationship (HQ Curve)

Pump pressure head (H), or the pressure gradient ( $\Delta P$ ) across the pump, is the pressure difference between the inlet and outlet ports of the pump. In the case of LVADs that pump from the LV to the aorta,  $\Delta P = \text{aortic pressure} - \text{LV pressure} + \text{combined pressure loss across the inlet cannula and outlet graft}$  [12]. At fixed operating speed,  $\Delta P$  dictates flow according to the pres-

sure-flow relationship, the so-called HQ curve, which is unique to each pump. Clinically, the relevant HQ curve is that of the entire system, which includes the pump, the inflow cannula, and the outflow graft [6].

HQ curves are typically generated in mock loops by measuring the pressure difference between the system inlet and outlet while gradually increasing resistance to outflow to the point of pump shutoff. Different curves are generated at different operating pump speeds and plotting  $\Delta P$  on the y-axis and pump flow on the x-axis [12]. However, from a physiological and clinical perspective, it is more appropriate to plot  $\Delta P$  on the x-axis (since this is the clinically independent parameter) and pump flow (the dependent parameter) on the y-axis. In general, cf-LVAD flow is inversely proportional to  $\Delta P$  as depicted for an axial-flow pump (HeartMate 2) in Fig. 5.1a [13] and for a centrifugal flow pump (HVAD) in Fig. 5.1b [9]. Axial-flow pumps tend to have relatively linear HQ curves, whereas the HQ curve of centrifugal pumps is more nonlinear.

During normal operation,  $\Delta P$  changes during the cardiac cycle, mainly due to cyclic variations of ventricular pressure during contraction (Fig. 5.2a). In systole, as the LV contracts, there is a reduction in  $\Delta P$ , and flow is at a maximum. During diastole, with LV relaxation,  $\Delta P$  increases, and pump flow decreases (Fig. 5.2b). Thus, due to the time-varying pressure gradient, pump flow also varies along the HQ curve with each cardiac cycle, even with a closed aortic valve [14, 15] (Fig. 5.2c, d). Accordingly, while flow from these pumps is continuous, it is not generally speaking, constant.

Significant differences can exist between centrifugal and axial-flow pumps that impact on the relative degrees of flow pulsatility for a given change in pressure, sensitivity to afterload resistances, and responses to suction [16, 10]. Importantly, differences between pumps do not result in major differences in clinical effectiveness since, in practice, RPMs are adjusted to provide the degree of support needed based on individual patient needs.



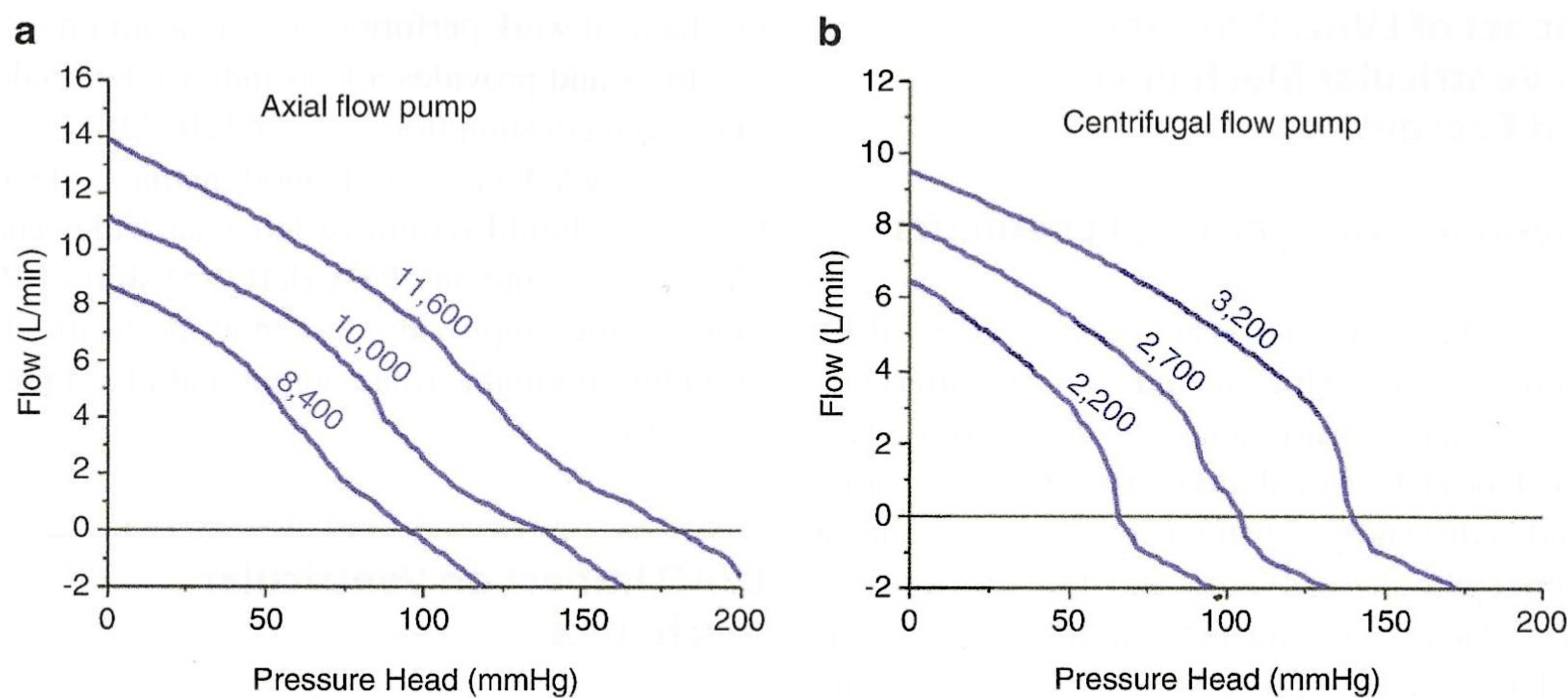


**Fig. 5.1** (a) HQ relationship representative of a HeartMate II axial-flow pump at three specified RPMs. (Created with Harvi-Online <http://harvi.online>) (b) HQ relationship representative of an HVAD centrifugal flow pump at three specified RPMs. (Created with Harvi-Online <http://harvi.online>)

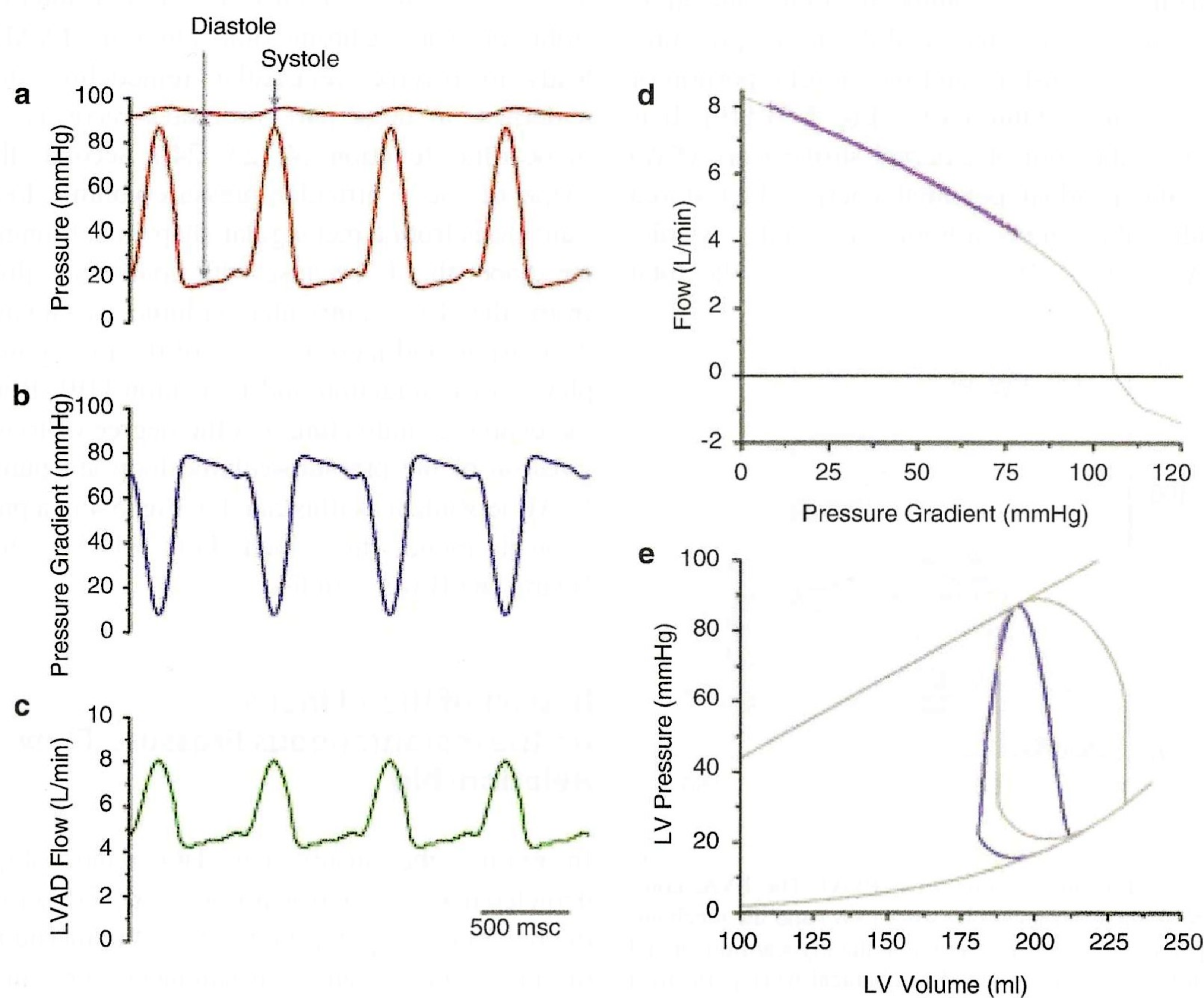


**Fig. 5.2** Variations of aortic and ventricular pressures during the cardiac cycle (a), the resulting time-varying pressure gradient across the pump inlet and outlet during the cardiac cycle (b), and resulting flow waveform (c). The flow waveform is determined by the time-varying pressure gradient as it projects onto the HQ curve at the

specified RPM (d). LVAD flow impacts on LV filling and mechanics as depicted on the pressure-volume diagram (e) which shows in comparison with pre-LVAD conditions (dark gray loop) a leftward shift and transition from rectangular to a triangular loop (blue) [19, 23]. (Created with Harvi-Online <http://harvi.online>)



## Impact of LVAD Pumping on Ventricular Mechanics and Energetics

### Physiology of Myocardial Energetics

Myocardial oxygen consumption is affected by multiple factors which include preload, afterload, muscle mass, heart rate, and contractility [17, 18]. Coronary blood flow (CBF) on the other hand is driven by a difference between the mean arterial pressure in diastole and downstream pressure related to the mean right atrial pressure as well as the left ventricular end-diastolic pressure (LVEDP) [17].

Pressure-volume analysis unifies the complex interactions listed above. Left ventricular pressure-volume area (PVA) is defined as the area on the pressure-volume diagram bounded by the end-systolic and end-diastolic pressure-volume relationships and the systolic portion of the pressure-volume curve (Fig. 5.3) [19]. It is equal to the sum of external stroke work (SW) plus the residual potential energy (PE) stored inside the myocardium at end systole:  $PVA = SW + PE$ . PVA is equal to the total

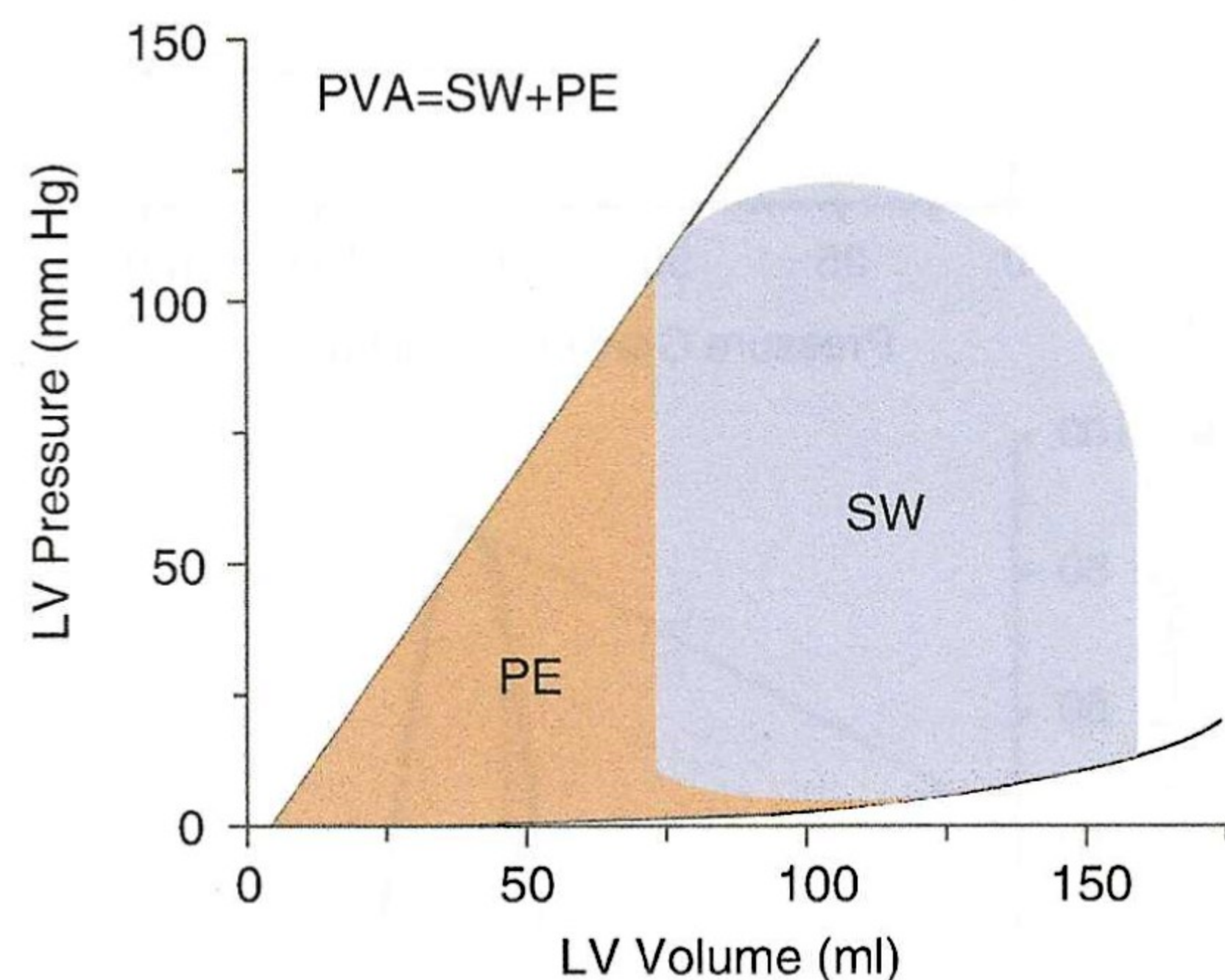


**Fig. 5.3** Pressure-volume area (PVA). The PVA, composed of the external stroke work (SW) and the mechanical potential energy (PE) stored in the myocardium at end diastole, represents the total mechanical work performed by the heart and correlates closely with total myocardial oxygen consumption per beat [19, 20]. (Reprinted from Burkhoff et al. [19], with permission from Elsevier)

mechanical work performed by the heart on each heartbeat and provides a load-independent index of oxygen consumption per beat [20–22].

Ideal VAD-assisted hemodynamic effects, therefore, should minimize left ventricular end-diastolic pressure and PVA (leftward shift of PV loop) while improving systemic perfusion by providing normal cardiac output and blood pressure [20].

### LVAD Impact on Ventricular Mechanics

Blood flow due to cf-LVADs impacts ventricular mechanics in several ways, which are readily appreciated on the ventricular pressure-volume diagram (Fig. 5.2e). First, pumping the blood directly from the LV reduces LV volume and diastolic pressure. Chronic unloading by LVADs leads to reverse ventricular remodeling that underlies, in large part, promotes recovery of myocardial function [4, 23, 24]. Second, the shape of the ventricular pressure-volume loop transitions from a rectangular shape to a triangular shape; this is because with continuous flow from the LV, ventricular volume is always decreasing, and there is a loss of the isovolumic phases of contraction and relaxation [19]. Both the degree of unloading and the degree of triangulation of the pressure-volume loop are pump RPM-dependent as illustrated in Fig. 5.4 in a pre-clinical model in which both HVAD and HeartMate II were studied.

### Impact of Blood Inertia on the Instantaneous Pressure-Flow Relationship

In reality, the steady-state HQ relationships depicted in Fig. 5.1a, b do not adequately describe the dynamics of pump flow due to the inertia of the blood which causes instantaneous pressure-flow relationships to deviate from the curves that are measured under steady-state conditions.



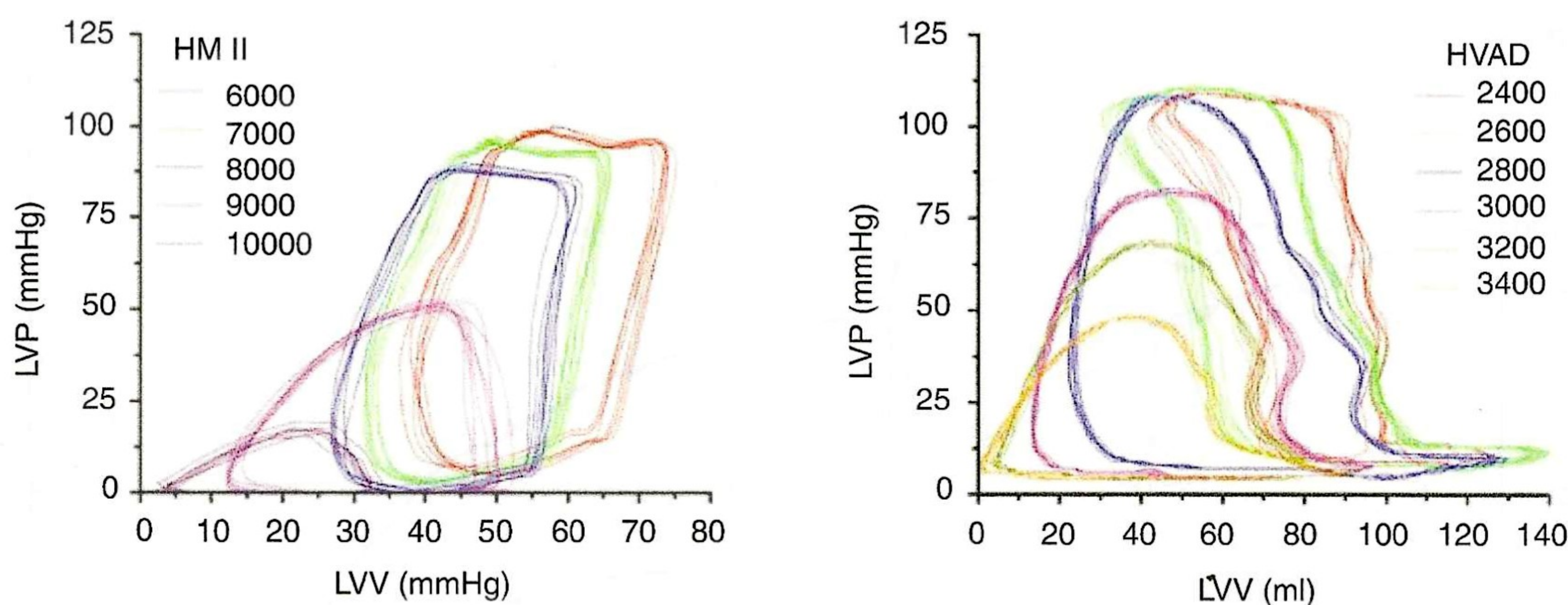


**Fig. 5.4** Pressure-volume loops from a preclinical model in which LVAD speed is gradually ramped. Baseline loops (without LVAD pumping) shown in red. As RPMs are increased for both HeartMate II and HVAD, the loops

shift progressively leftward toward lower volumes (dose-dependence of unloading) and become increasingly triangular. (Created with Harvi-Online <http://harvi.online>)

Using mock circulatory loops coupled with a pneumatic mock ventricle, several studies have demonstrated that the instantaneous LVAD pressure-flow relationship deviates from the steady-state HQ curves, demonstrating hysteresis as illustrated in Fig. 5.5 [25, 26]. We can further define the impact of inertia and hysteresis on overall function using *in silico* modeling [27] as illustrated in Fig. 5.6. The presence of inertia (and thus hysteresis around the steady-state curve, (Fig. 5.6a, b) decreases peaks and troughs of the flow waveform (Fig. 5.6c), thus decreasing intrinsic VAD flow pulsatility, but, interestingly, does not substantially impact on the average flow and insignificantly impacts on the LV pressure-volume loop (Fig. 5.6d).

### Pump Power and Flow Relationship

For centrifugal pumps, there is a reasonably linear relationship between the electrical power drawn and the flow generated by the pump. Accordingly, flow estimates provided by pumps such as the HVAD which are based on established lookup tables which relate RPMs, blood viscosity (related to hematocrit), and electrical power to flow are considered reasonably reliable [28, 29]. In contrast, axial-flow pumps exhibit a

nonlinear, U-shaped relationship between electrical current and flow [6]. Under this circumstance, flow estimates are considered less reliable.

### Artificial Flow Pulsatility

As detailed above, flow from cf-LVADs varies with ventricular contraction and therefore can introduce a degree of arterial pressure pulsatility even if the aortic valve does not open. Based on the explanations above, intrinsic pulsatility due to ventricular contraction depends on the slope of the HQ curve [15]. The degree of pulsatility has been indexed clinically by the pulsatility index (PI) which is calculated and displayed in different ways for different pumps. For HeartMate II and III, PI is calculated as beat-to-beat amplitude between the maximal flows and minimal flows averaged over 10–15 seconds and divided by the average flow according to the formula: (maximum flow – minimum flow)/average flow. In HVADs pulsatility is displayed as real-time waveforms (Fig. 5.7). PI is inversely related to speed under conditions of constant preload and afterload [11].

Due to the potential physiological importance of pulsatility, several devices incorporate algorithms to vary RPMs to artificially introduce additional pulsatility; the clinical benefits



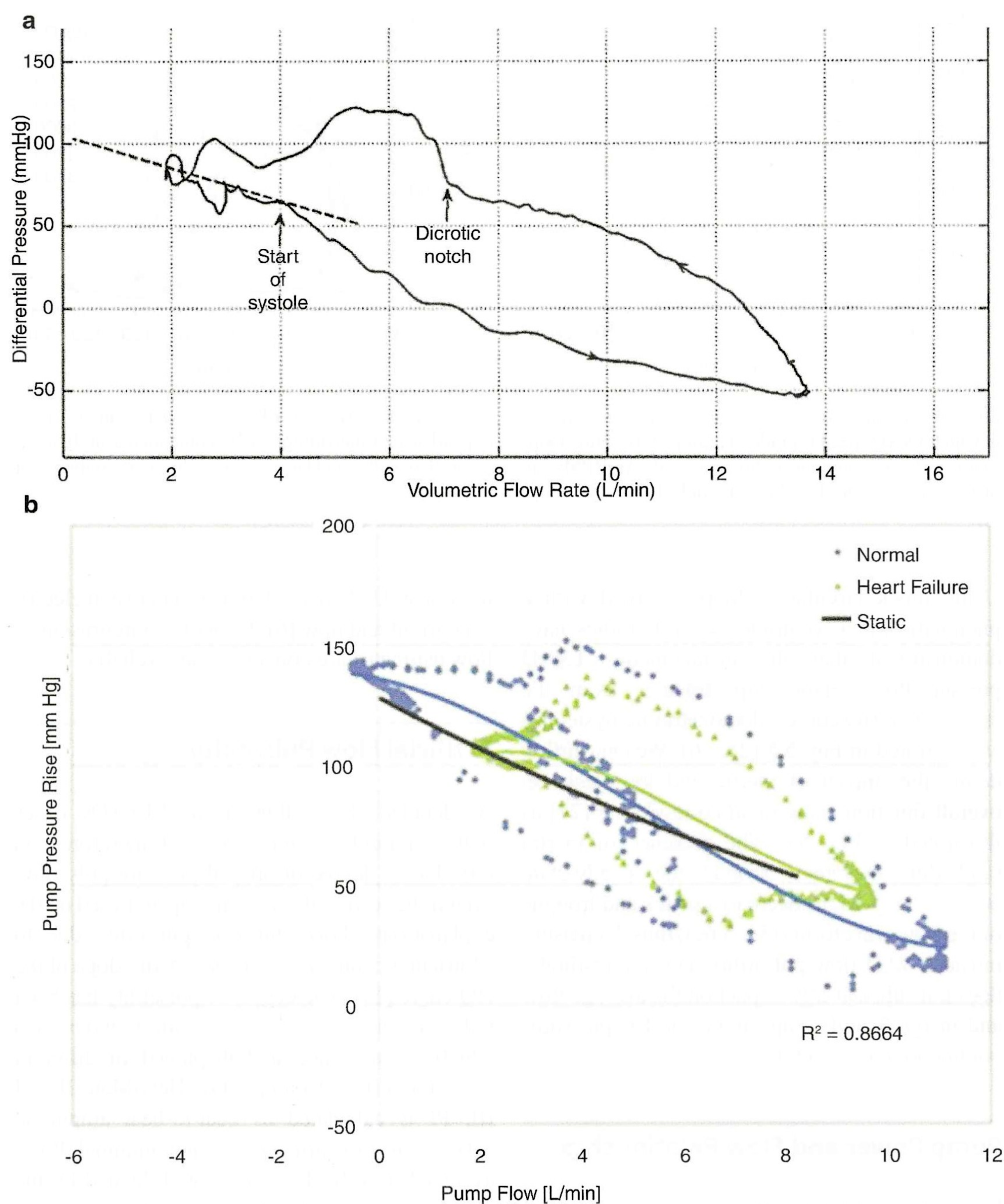


**Fig. 5.5** HeartMate II instantaneous HQ (flow-pressure) loops measured in mock loops showing hysteresis around the steady-state relationship. (a) Study by Noor et al. [26]. (Reprinted from Noor et al. [26], with permission from

John Wiley and Sons). (b) Study by Sunagawa et al. [25]. (Reprinted from Sunagawa et al. [25], Copyright (2015), with permission from Elsevier)

of such artificial pulsatility remain controversial [30, 31]. Purported advantages of pulsatile circulation in VAD patients include decreased

blood stasis in the ventricle, intermittent aortic valve opening, decreased risk of ventricular suction by allowing intermittent LV filling, and



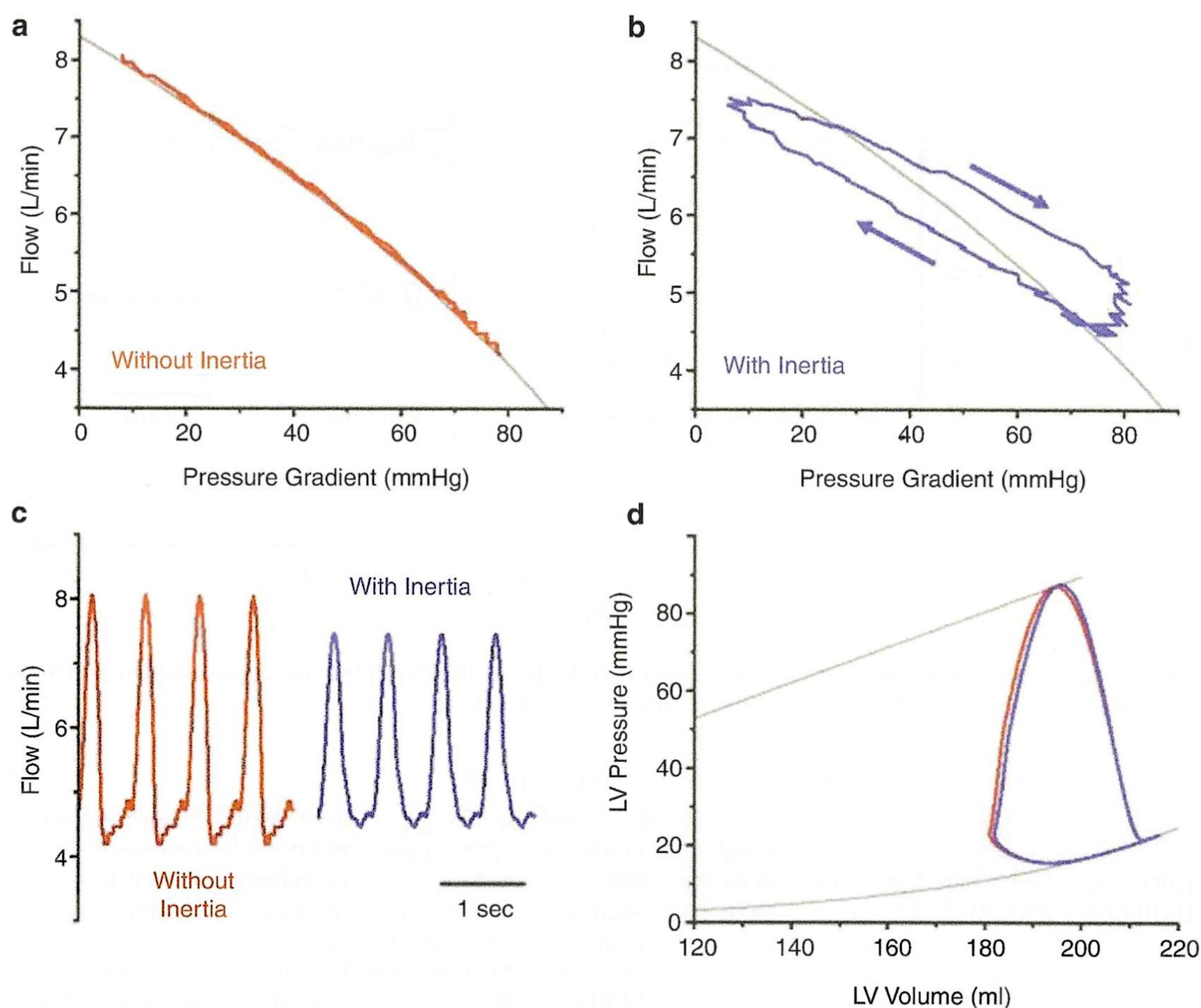


**Fig. 5.6** Simulation model [27] showing the impact of inertia on the instantaneous LVAD pressure-flow relationship. (a) Without inertia, the instantaneous LVAD pressure-flow relationship follows the steady-state curve (gray). (b) With inertia added to the model, the loop deviates from the steady-state curve in a manner similar to that

observed experimentally (as in Fig. 5.5). (c) The instantaneous flow signal pulsatility is decreased by the presence of inertia, but the mean flow is not significantly impacted. (d) Despite the impact of inertia on the flow signal, the impact on the ventricular pressure-volume loop is insignificant. (Created with Harvi-Online <http://harvi.online>)

potentially beneficial effects on end-organ function [32]. Some studies indicate pulsatile flow maintains lymphatic flow, decreases systemic vascular resistance [33], and improves autonomic function [34].

Accordingly, some cf-LVAD (e.g., HVAD and HM III) have an artificial pulse mode which induces pulsatile flow by transiently and rapidly varying pump speed [9]. HVAD has a so-called Lavare cycle that has been in place outside of the US for some time and more recently introduced in the US [35]. Benefits of this algorithm and pulsatility, in general, have not been definitively established.

## Impact of RPMs on LVAD Flow and Total Flow to the Body

### Ramp Test

One of the challenges faced in the care of LVAD patients is understanding how to optimally set the RPMs. Ideally, speed would be adjusted to simultaneously achieve normal values of filling pressures (both CVP and PCWP), arterial pressure, and total blood flow to the body. Unfortunately, this is not always possible simply by adjusting speeds, and medical management is required for adjustment of arterial resistance and



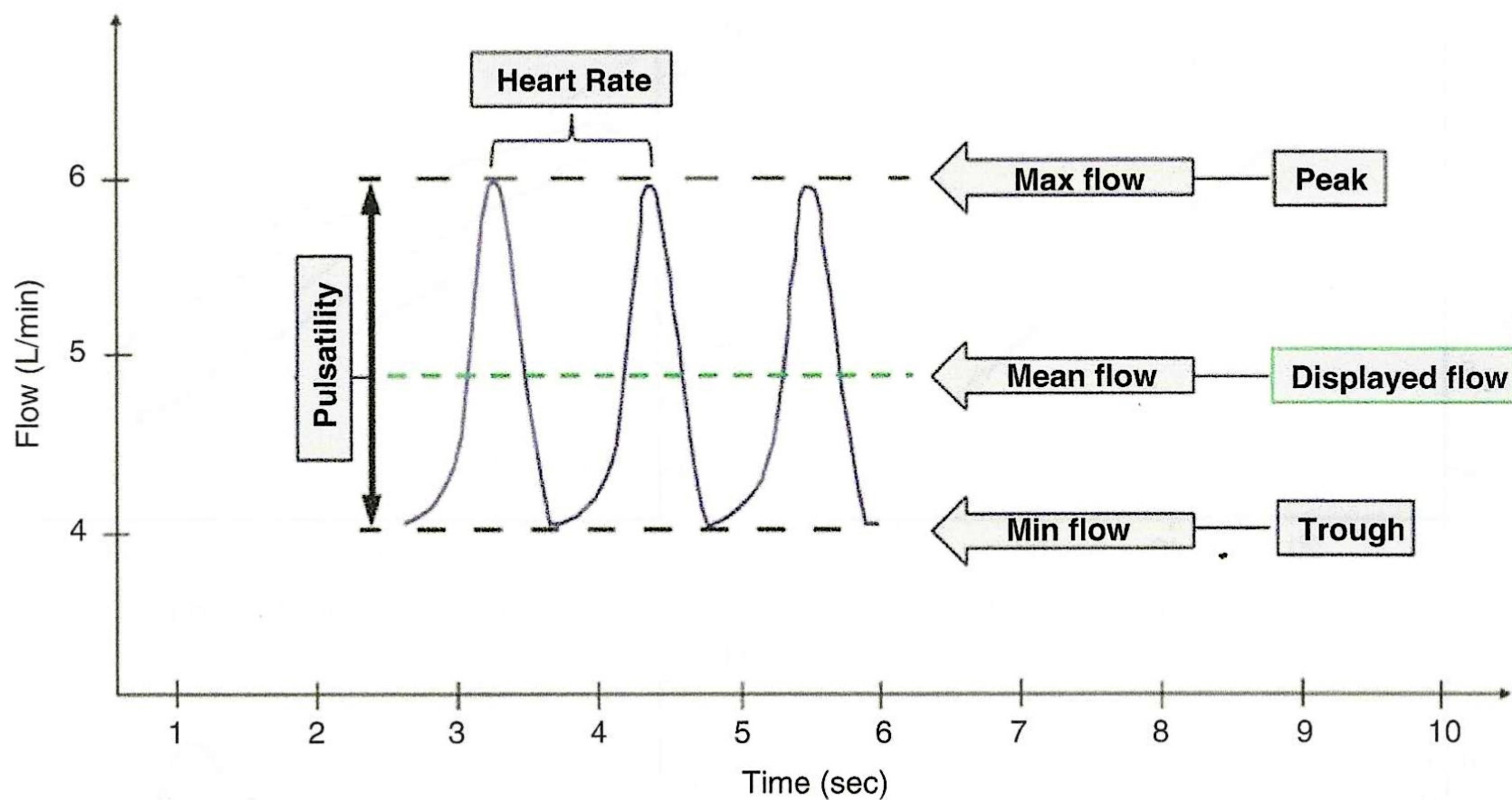


**Fig. 5.7** A typical HVAD waveform [28]. (Reprinted from Rich and Burkhoff [28], <https://journals.lww.com/asaio-journal/pages/default.aspx> with permission from Wolters Kluwer Health, Inc)

**Table 5.1** Characteristics of axial and centrifugal-flow pump ramp tests

pump	Lower rate	Upper rate	Speed increment	Parameters to stop the test	Device optimization goals	Features of pump thrombosis	Parameter slopes for device malfunction
HMII [38]	8000 RPM	12,000 RPM	400 RPM	Suction event (and/or) LVEDD <3.0 cm	Intermittent AV opening MAP >65 mm Hg MR not more than mild in severity	Minimal change in LVEDD with an increase in pump speed Clinical parameters: ↑LDH	LVEDD slope > -0.16 rpm/increment (regardless of AV closure) LVEDD slope (varies with aortic valve closure) Open AV valve LVEDD slope > -0.09 rpm/increment Closed AV valve LVEDD slope > -0.15 rpm/increment
HVAD [39]	2300 RPM	3200 RPM	100 RPM				

**Abbreviations:** LVEDD left ventricular end-diastolic dimension, AV aortic valve, RPM revolutions per minute, MAP mean arterial pressure, MR mitral regurgitation, LDH lactate dehydrogenase

fluid status. Understanding of the complex interactions between the LVAD and body properties has been enhanced through the use of speed ramp tests.

More specifically, hemodynamic speed ramp tests in cf-LVADs can be used to assess the dynamic interactions between device speed, left and right ventricular filling pressures (PCWP and CVP, respectively), as well as valve func-

tion using invasive pulmonary artery and echocardiographic methods. Ramp tests are used in the initial postoperative care of cf-LVAD patients to determine the appropriate LVAD speed [36] and also in stable LVAD patients to optimize hemodynamic conditions through speed and medication adjustments [37] as well as diagnose device malfunction and need for surgical or conservative interventions. Table 5.1



describes the characteristics of ramp tests for HeartMate II and HVAD devices, devices for which most information is currently available.

### HeartMate II Echocardiographic Ramp Test

Uriel et al. defined a systematic approach to perform and analyze hemodynamic ramp tests [38]. The ramp test protocol for axial-flow pump (HM II) is performed by reducing the RPM of the pump to 8000 RPM and measuring left ventricular end-diastolic dimension (LVEDD), left ventricular end-systolic dimension (LVESD), frequency of AV opening, degree of AR, degree of mitral regurgitation (MR), right ventricular systolic pressure (RVSP), Doppler blood pressure, heart rate, pump power, pulsatility index (PI), and pump flow. Subsequently, the speed is increased by 400 RPM at 2-minute intervals, and all measurements are repeated until the pump reaches 12,000 RPM or the maximum tolerable speed. The ramp test is stopped if there is a suction event or if the LVEDD decreases to less than 3 cm. Pump thrombosis can be diagnosed when there is minimal change in the LVEDD with an increase in pump speed. The slope of RPM-LVEDD correlates with pump thrombosis or severe outflow obstruction due to an uncoupled relationship between increases of pump speeds and decreases in LVEDD. For HM II, an RPM-LVEDD slope  $> -0.16$  rpm/increment is significant for device malfunction.

### HVAD Echocardiographic Ramp Test

Ramp studies performed in a centrifugal pump (e.g., HVAD) is similar to that of an axial-flow pump ramp-study protocol. However, given differences in pump operating speeds, the ramp test (HVAD protocol) is started at 2300 rpm. Subsequently, the speed is increased in steps of 100 rpm to a max of 3200 rpm. Criteria for stopping the ramp studies are the same as detailed

above [37]. The parameter slopes for HVAD are significantly different from HMII and vary with the aortic valve (AV) status. With AV valve open, the RPM-LVEDD slope for device malfunction was  $> -0.09$  rpm/increment and with closed AV  $> -0.15$  rpm/increment [39].

Invasive ramp tests with the use of a pulmonary artery catheter to assess CVP and PCWP can provide a more detailed assessment of the underlying hemodynamic state [37, 40]. Doppler-TTE-derived variables from the LVAD outflow graft were also recently shown to predict PCWP, CO, and SVR reliably and could potentially reduce the need for invasive testing [41]. Ramp tests in stable LVAD patients are reproducible and may represent a hemodynamic fingerprint for a patient. Changes in the ramp test can be used to assess device malfunction or alterations in volume status, peripheral vascular resistance and offer an opportunity to optimize medication doses and device settings [40].

### Impact of RPM on Left Ventricle

Cf-LVADs pump blood continuously from the LV to aorta independent of the cardiac cycle. As a result, there is a loss of normal isovolumetric periods, and the PV loop morphology changes to a triangular shape from the normal rectangular or trapezoidal shape. With further increases in RPMs, the LV becomes progressively unloaded, and the PV loop shifts to the left (Fig. 5.8a). The leftward shift signifies a reduction in peak LV pressure generation and marked reduction in PVA and MVO<sub>2</sub>. As the degree of unloading increases, there is an increasing dissociation between aortic and left ventricular pressures (Fig. 5.8b–e).

### Impact of RPM on Total Body Flow

While LVAD flow increases with an increase in RPMs, increases in RPM do not always result in increased overall flow to the body as detailed in Fig. 5.9. With the initiation of LVAD flow, LVAD



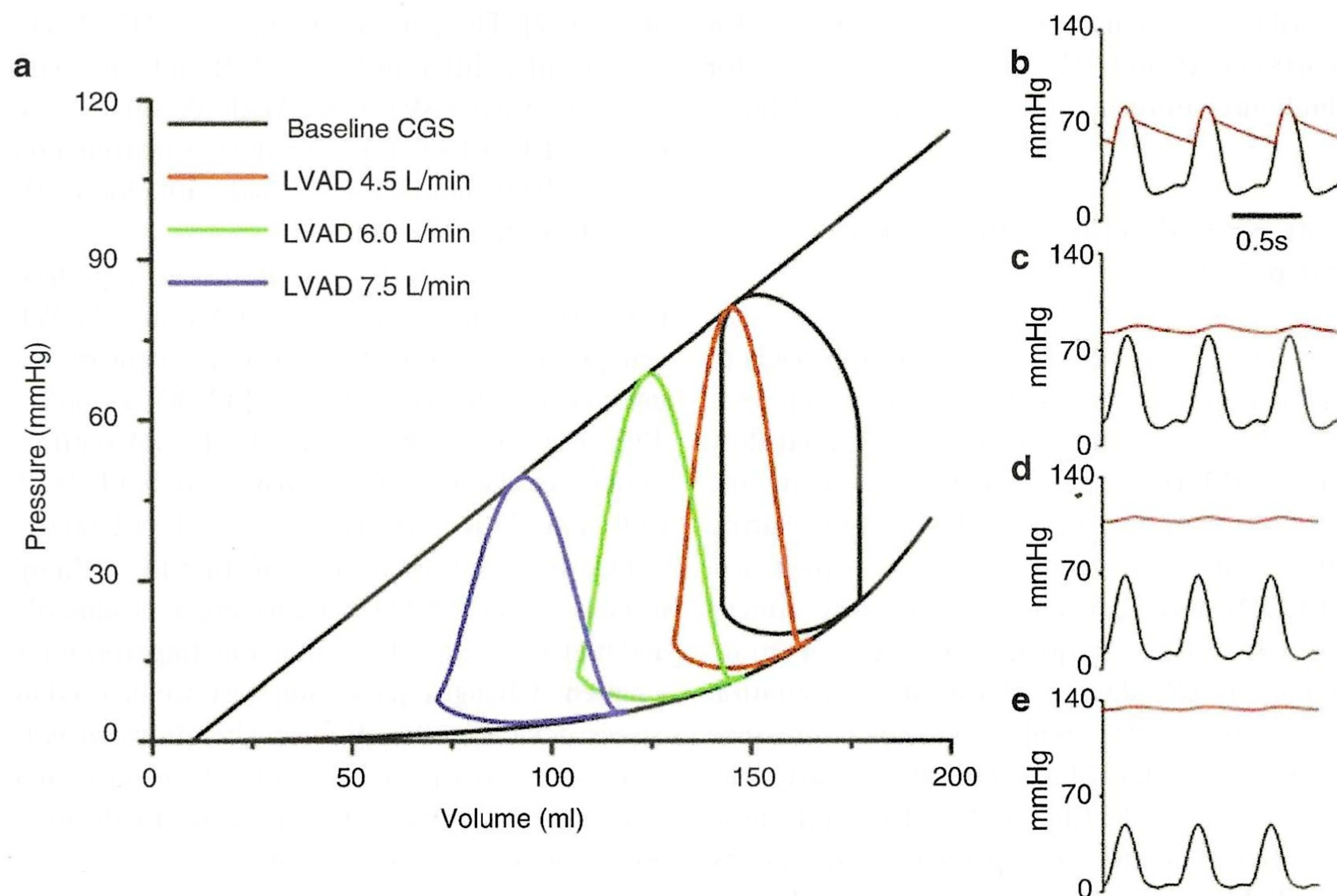


**Fig. 5.8** Impact of RPM on the left ventricle. (a) Progressive unloading of the left ventricle with leftward shift of the PV loop. (b–e) Increasing dissociation can be noted between LV and aortic pressures with a progressive

increase in the degree of LV unloading [19]. (Reprinted from Burkhoff et al. [19], Copyright (2015), with permission from Elsevier)

flow will unload the LV and increase afterload pressure, thus reducing intrinsic CO from the heart. As RPMs are increased, LVAD flow progressively increases, and intrinsic CO decreases. While RPMs are within a range where part of the flow is from the heart and part of the flow is from the LVAD is said to be providing *partial support*. Thus, within this range, while LVAD flow is increasing significantly with RPM increments, total flow seen by the body increases, but by a smaller amount. At some point, aortic pressure increases such that the LV no longer ejects and the aortic valve remains closed. After this point, total flow seen by the body is only provided by the pump; this is *full support* condition, and the slope of the curve relating RPMs to total flow increases.

From a terminology perspective, it is also important to distinguish between the degree of support and the degree of LV unloading

(Fig. 5.10). As detailed in the next section, full support and full unloading are not synonymous.

### Defining and Quantifying Ventricular Unloading

Promotion of ventricular reverse remodeling depends on adequate LV unloading and achieving VAD-assisted ideal hemodynamic state [42]. *LV unloading* has been defined as the reduction of total mechanical power expenditure ( $PVA \cdot HR$ ) of the ventricle which correlates with reductions in myocardial oxygen consumption and hemodynamic forces that lead to ventricular remodeling [19, 23]. Full unloading, therefore, only occurs when PVA has reached a minimal value (Fig. 5.10, rightmost panel). In contrast, as detailed above, *full support* occurs when there is uncoupling of arterial pressure and left



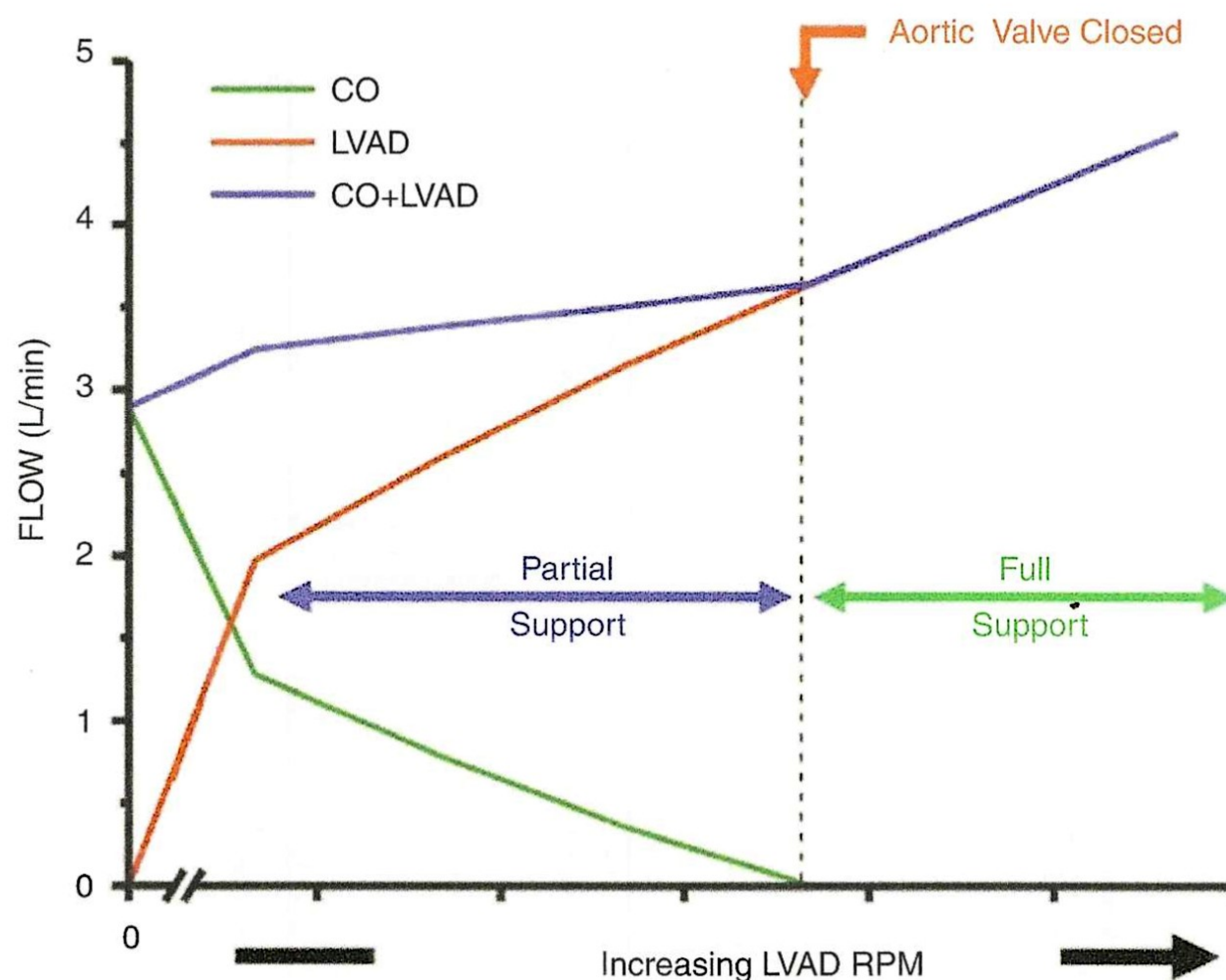


**Fig. 5.9** Impact of LVAD speed on LVAD flow, intrinsic cardiac, and total flow to the body ( $=CO+LVAD$ ). With the initiation of LVAD flow, LVAD flow will unload the LV and increase afterload pressure, thus reducing intrinsic CO from the heart. As RPMs are increased, LVAD flow progressively increases, and intrinsic CO decreases. This is a *partial support* condition in which part of the flow is

from the heart and part is from the LVAD. Total flow seen by the body increases, but by a smaller amount. At some point, aortic pressure increases such that the LV no longer ejects and the aortic valve remains closed. After this point, total flow seen by the body is only provided by the pump. This is *full support* condition. (Created with Harvi-Online <http://harvi.online>)

ventricular systolic pressure resulting in a closed aortic valve [9]. Thus, full support can be achieved, while the LV is only minimally unloaded (middle panels, Fig. 5.10). Clinically, significant mitral regurgitation can also signify inadequate unloading. Pulsatile first-generation pumps running on the eject-on-full mode offered profound LV unloading [43]. There is conflicting evidence about the equivalence of LV unloading with pulsatile VADs vs. cf-LVADs, although both can offer adequate hemodynamic support [7, 43, 44].

### Impact of RPM on CVP and PCWP

Assessment of complex VAD-ventricular interactions based on physical examination can be challenging, in particular as it relates to assessing an LVAD patient's volume status. In a study evaluating the use of invasive hemodynamic

ramp test for device optimization in clinically stable cf-LVAD patients, at baseline, only 43% of the patients had normal CVP and PCWP at their original RPM settings (Fig. 5.11). During the ramp test, with an increase in speed, cardiac output increased, and PCWP decreased with no significant change in the CVP and SBP. 56% of the patients required adjustment of their pump speed from its original setting to achieve CVP and PCWP close to normal range [37]. Finally, in a large percentage of the patients studied, CVP and PCWP could not be optimized, signifying the need for altered medical therapy (diuretics and/or afterload reduction). The finding that there was no rpm-dependent change in CVP suggested the beneficial impact of LV unloading on RV function [37]. The findings were similar in patients supported by HM2 and HVAD. The conclusion of the study is that clinical assessment of volume status in LVAD patients is very challenging, and the hemody-



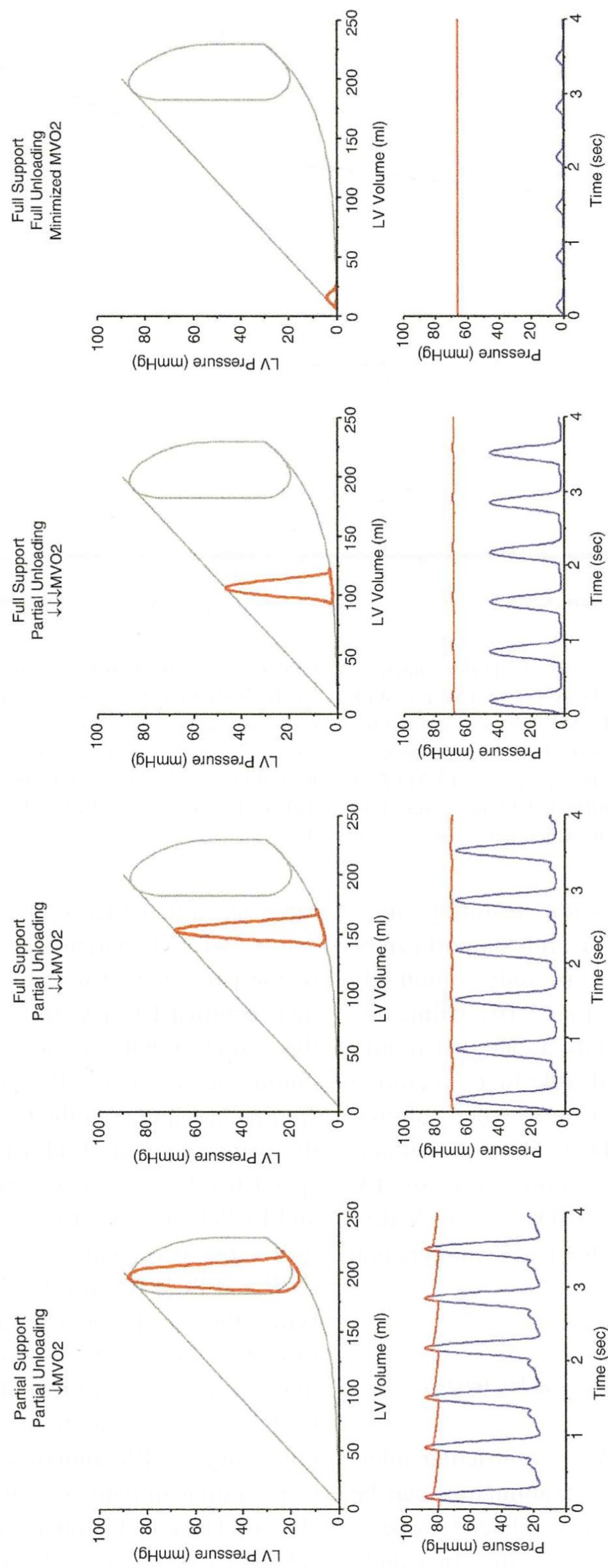


**Fig. 5.10** Degree of support versus degree of unloading. (Created with Harvi-Online <http://harvi.online>)



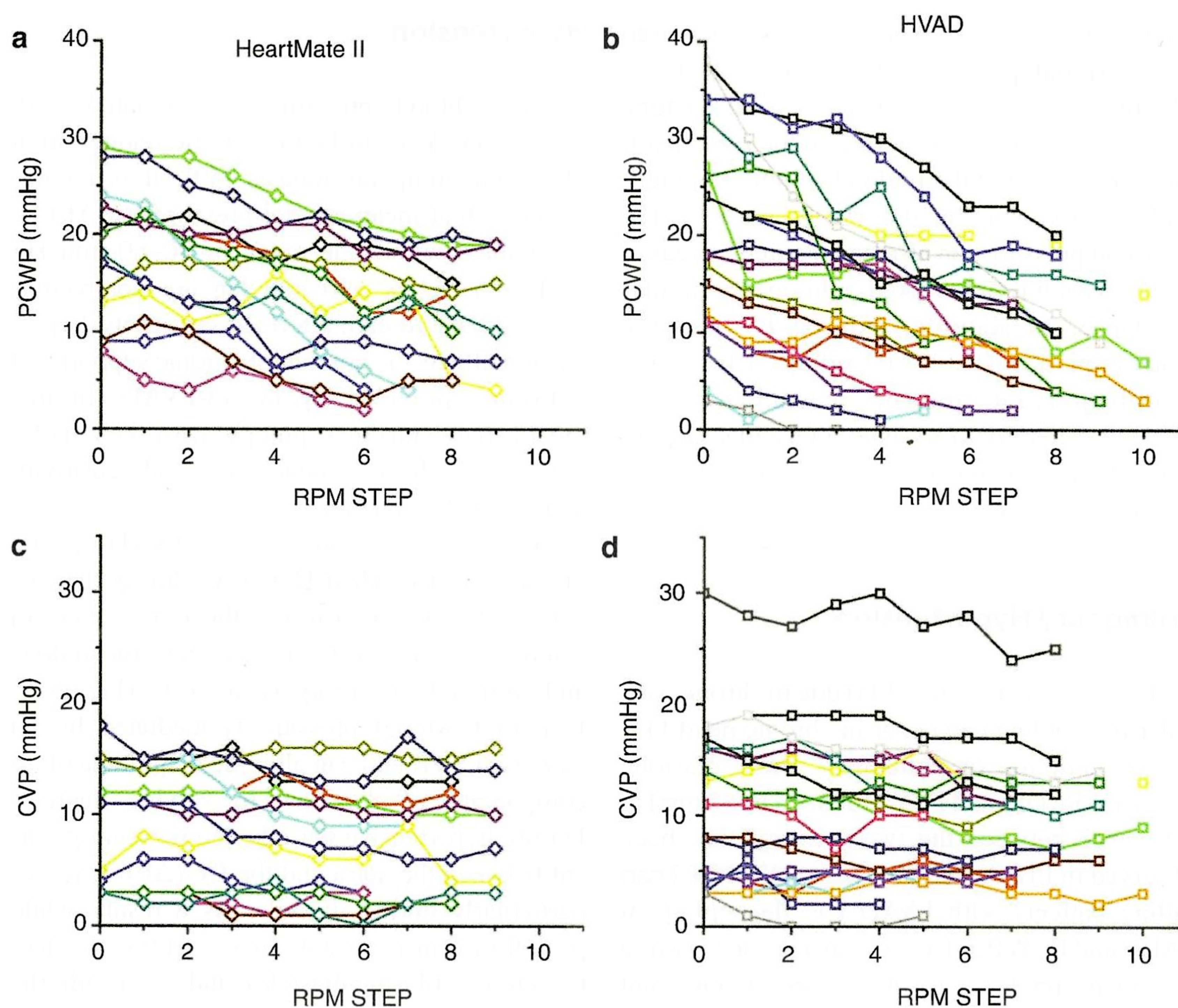


**Fig. 5.11** Impact of LVAD RPMs on pulmonary capillary wedge pressure (PCWP) and central venous pressure (CVP) in patients supported by either HeartMate II or

HVAD [37]. (Reprinted from Uriel et al. [37], Copyright (2016), with permission from Elsevier)

dynamic ramp tests can be helpful not only in determining optimal speed setting but perhaps more importantly for adjusting medical therapy, particularly diuretic dosing.

## Special Considerations

### RV Failure with LVAD

Right heart failure is an important problem encountered in patients undergoing LVAD support. It occurs with a frequency of ~20–25% in the perioperative period, with ~1–5% of patients

requiring at least temporary mechanical right ventricular support. In recent studies, approximately 30% of patients experience right heart failure during chronic LVAD support. Hemodynamic and mechanical interaction between right and left heart occurs due to their connection in series and anatomical coupling from a shared interventricular septum. LVADs can have either a beneficial or a detrimental effect on RV function. Beneficial effects can include a decrease in RV afterload (i.e., reduction of PCWP), favorable alteration of the RV geometry due to a reduction in impingement of the RV by the interventricular septum, as well as



improved coronary flow as a result of increased mean arterial pressure. Deleterious effects on RV function can result from several factors. LVADs increase venous return to the right heart, thereby increasing the preload which can potentially overwhelm the RV. An increase in RV afterload pressure can also occur when increased flow passes through a fixed pulmonary vascular resistance. In addition, reduced LV pressure generation due to LV unloading reduces LV contribution to RV pressure generation, and the effect is referred to as interventricular dependence that is mediated mainly by the interventricular septum [45].

### Pulmonary Hypertension

Pulmonary hypertension (PH) due to chronic vascular remodeling can occur in chronic heart failure. Decoupling of pulmonary artery diastolic pressure (PADP) and PCWP defined as  $>5$  mmHg difference between the two pressures has been observed in PH. A study reports of 43–48% heart failure patients with LVAD had decoupling of PADP and PCWP at baseline speeds, and it was a significant predictor for the composite endpoint of death and heart failure readmissions. 30% of the patients with decoupling could be normalized after a combined invasive hemodynamic measurement and ramp test-based change in the device setting. Normalization was significantly associated with 1 year heart failure readmission-free survival compared to non-normalized group [46].

### Clinical LVAD Physiology

Understanding ventricle-VAD interaction enables identification of clinical pathology especially when flow waveforms are available as detailed by Drs. Rich and Burkoff [28]. Table 5.2 summarizes common pathologic conditions and VAD responses.

The concept is illustrated by one of these conditions: the detection of hypertension is of particular relevance.

### Hypertension

Elevated blood pressure is associated with increased risk of stroke [47], aortic regurgitation [48], and pump thrombosis [49]. It is recommending that mean arterial pressures (MAP) be maintained within the range of 70–80 mm Hg [36], and MAPs  $>90$  mm Hg are not recommended. Due to high afterload sensitivity, hypertension affects the amount of cardiac support and unloading provided by the cf-LVAD. In this regard, the centrifugal pumps, with their flatter H-Q curves, have a higher afterload sensitivity than axial-flow pumps.

As detailed previously, the cf-LVAD operate on the rpm-dependent HQ curve during the cardiac cycle, and, as a result, the flow waveform can be characterized by its peak flow, mean flow, and trough flow during each cycle (Fig. 5.7). Increased arterial pressure is mediated by an increased SVR and can alter the magnitude of all components of the flow to varying degrees. During hypertensive periods, the pressure gradient between the aorta and the LV ( $\Delta P$ ) increases particularly during diastole. As a result, while peak flow (during systole) may be little affected, trough flow (during diastole), and as a result, the mean flow, can be markedly reduced depending on the degree of elevation of the arterial pressure; this is associated with a significant increase in pulsatility (Fig. 5.12a). In certain circumstances, either no diastolic flow and even negative flow or flow reversal can occur [25, 50].

The opposite situation occurs in a patient who is hypotensive (Fig. 5.12b). In such a case,  $\Delta P$  is lower than normal, and there is less variability of pressure gradient. Accordingly, mean flow is increased, and flow pulsatility is decreased.

### VAD-Exercise Physiology

Aerobic exercise in healthy individuals results in increased heart rate, increased stroke volume, decrease in systemic vascular resistance, and mild to moderate elevation in blood pressure without elevation in intracardiac filling pressures. Whereas in heart failure, stroke volume is



**Table 5.2** Common pathologic conditions and VAD responses [28]

Condition	Loading conditions for the pump	$\Delta P$ systole	$\Delta P$ diastole	Speed	Power	Flow	Pulsatility	Hemodynamic parameters
Hypovolemia	Decreased preload	↑	↑	Constant	Low	Low	Low	CVP ↓ PCWP ↓ CO ↓
Hypervolemia	Increased preload	↓	↓	Constant	High	High	High	CVP ↑ PCWP ↑ CO →
RV failure	Decreased preload	↑	↑	Constant	Low	Low	Low	CVP ↑ PCWP ↓ CO ↓
Moderate hypertension	Increased afterload	↑	↑↑	Constant	Low	Low	High (systolic predominant flow)	—
Severe hypertension	Increased afterload	↑↑	↑↑	Constant	Low	Low	Low (reduced flow in systole and diastole)	PCWP ↑
Outflow obstruction	Increased afterload	↑	↑	Constant	Low	Low	Variable	PCWP ↑ CO ↓
Inflow obstruction	Decreased preload	↑	↑	Constant	Low	Low	Variable	PCWP ↑ CO ↓
Relative Low pump speed	—	—	—	Low	Low	Low	High	PCWP ↑ or → CO ↓
Relative high pump speed	—	—	—	High	High	High	Low	PCWP ↓ CO ↑
Sepsis/vasodilation	Decreased afterload	↓	↓	Constant	High	High	Low	PCWP ↓ CO ↑
LV recovery	—	↓	↑	Constant	High	High	High	PCWP ↓ CO ↑
Pump thrombosis	—	—	—	Constant	High (power spikes)	High (overestimation)	Variable	CO ↓
Aortic insufficiency	Increased preload, Decreased afterload	↓	↓	Constant	High	High	Low	PCWP ↑ CO ↓
Tamponade	—	↑	→	Constant	Low	Low	Low	CO ↓

Abbreviations: CVP central venous pressure, PCWP pulmonary capillary wedge pressure, CO cardiac output, LV left ventricle, RV right ventricle



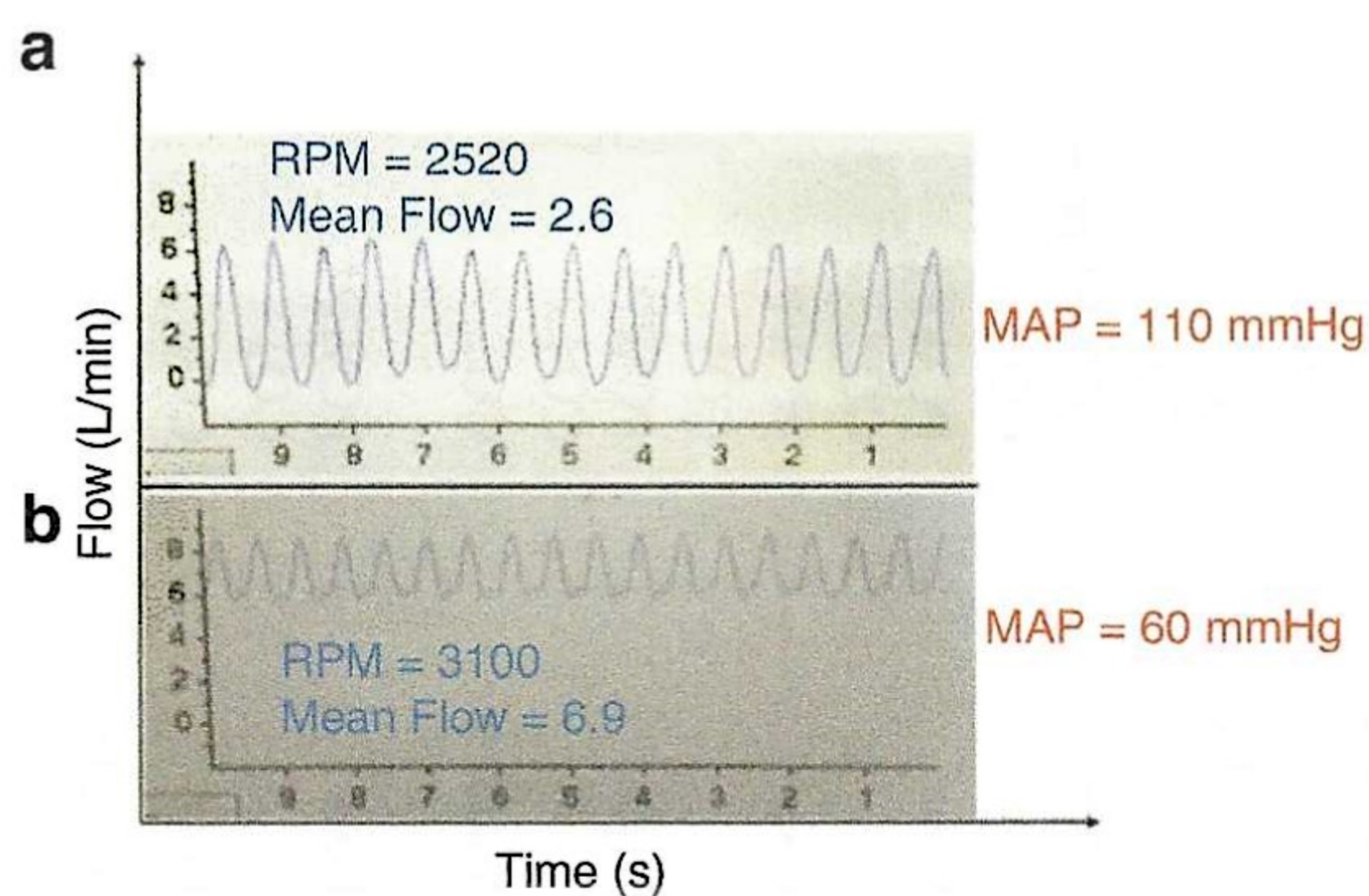


**Fig. 5.12** (a) Typical waveforms for a hypertensive patient (low flow, high pulsatility). (b) Flow waveform for a hypotensive patient (high flow, low pulsatility) [28]. (Reprinted from Rich and Burkoff [28], <https://journals.lww.com/asaiojournal/pages/default.aspx>, with permission from Wolters Kluwer Health, Inc)

increased at the expense of LVEDV [51, 52]. Hemodynamic responses to exercise in cf-LVADs are yet to be thoroughly characterized. At rest, LVADs improve hemodynamics, functional capacity, and ventilatory function. However, during exercise, despite hemodynamic support provided by LVAD, patients are unable to reach age- and sex-predicted normal aerobic capacity, and exercise performance is reduced by half the expected value [53, 54]. The reduction in functional capacity during exercise is multifactorial [53, 54]. No difference in hemodynamic support and exercise capacity has been noted between pulsatile and cf-LVADs [7].

### Hemodynamic Factors Affecting VAD Flow During Exercise

The optimal setting for cf-LVADs (described in ramp tests) permits intermittent AV opening. As a result, at rest, majority of the CO is maintained by the VAD. During exercise, an increase in heart rate, total cardiac output, mean systemic arterial pressure, mean PA pressure, wedge pressure, right atrial pressure, minute ventilation, and LVEDV has been reported [52].

As the native LV and VAD work as two pumps in parallel, any change in the filling pressure has a simultaneous effect on flows through both the

pumps. Jerson et al. showed that pump flow during exercise increases initially and later stabilizes at a moderate level despite a gradual increase in total cardiac output until maximum exercise suggesting an increased contribution from the native ventricle [13]. Physiologically this can be explained as follows: an increase in LV filling pressures causes a reduction in pump  $\Delta P$ , and pump flow increases through the VAD. At the same time, increase in preload and end-systolic elastance invokes the Frank-Starling relationship and facilitates opening of the aortic valve and ejection of the blood from the LV. On PV loops the effect of exercise at constant RPM results in a change from triangular shape of the loop at rest to a more trapezoidal shape with exercise (Fig. 5.13) [52]. With both pumps working in parallel, an initial increase in CO along with MAP is noted. The elevated MAP results in an increased  $\Delta P$  across the pump and prevents further increase in pump flow [13].

### Chronotropic Incompetence and Preload

The ability to augment heart rate plays a major role in augmenting stroke volume in healthy patients and has been associated with decreased exercise performance in heart failure [55]. The importance of chronotropic incompetence in patients with cf-LVAD is controversial. Early studies in calves showed that at fixed pump speeds, LVAD flow occurred predominantly in systole in exercise and was caused by an increase in the heart rate [56]. However, recently, Muthiah et al. [57] have demonstrated that changes in maximum and minimum heart rates by adjusting the pacemaker function did not show a significant change in cardiac output through the VAD in patients with closed AV valves. In contrast, changes in preload was associated with significant changes in the LVAD flow in the same set of patients as evaluated by tilt table testing. This was further supported in a study by Hu et al. [58] wherein recumbent position and not heart rate was associated with increased pump flow suggesting that preload plays a key role during exercise.



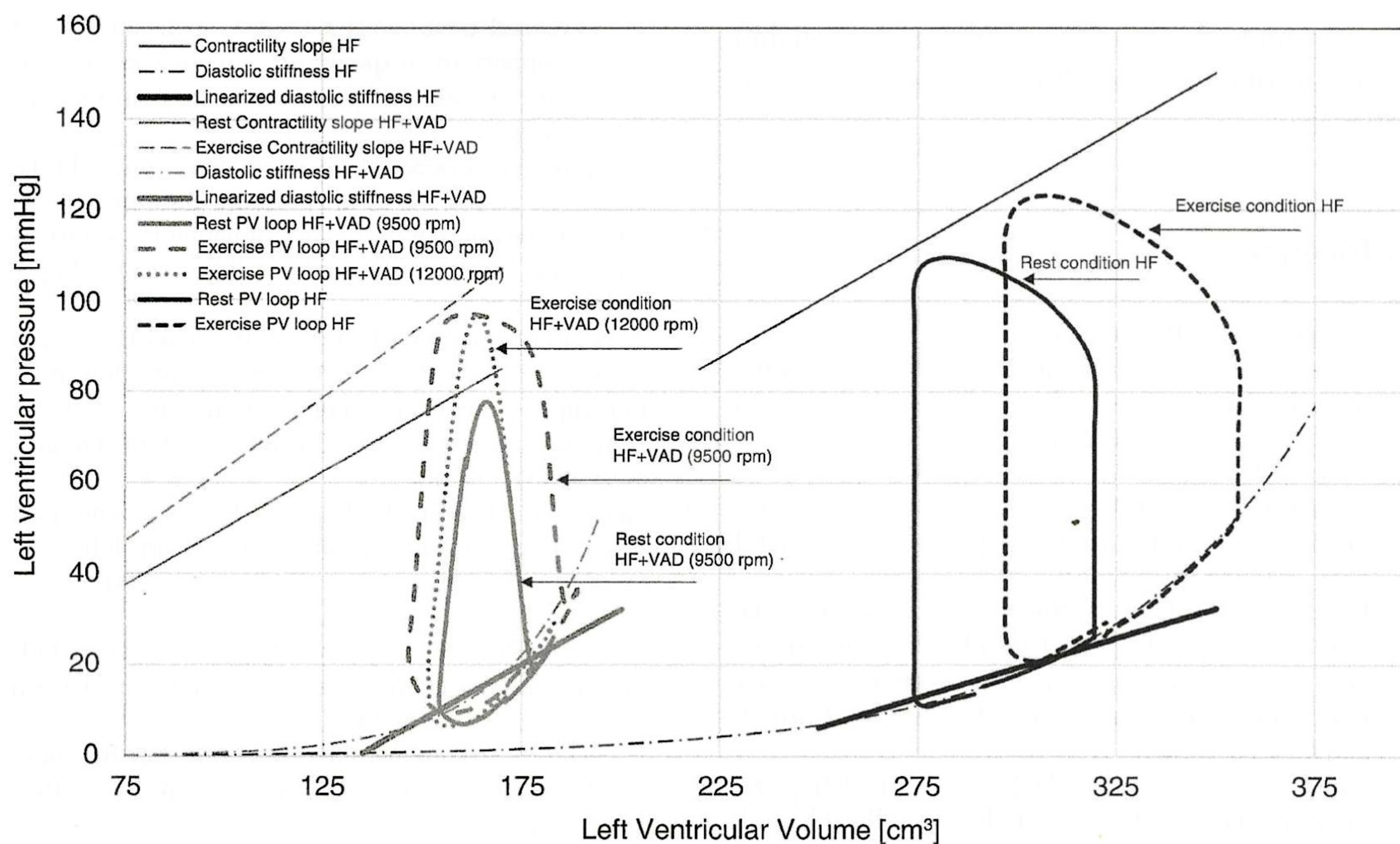


**Fig. 5.13** Physiology of exercise in a heart failure patient versus an LVAD patient at different RPMs. (Reproduced under an open access license (CC BY) [52])

### Effect of Pump Speed Adjustment During Exercise

In current practice, cf-LVADs are run at fixed RPMs irrespective of the level of activity. Several studies have assessed the role of active pump modulation with mixed results [59, 60]. No significant benefit of increasing pump speed during exercise in terms of total cardiac output has been reported in recent literature [61, 62]. On the contrary, increased in PCWP and RAP during exercise were noted, even with increased speed [52, 62, 63]. The likely explanation for this phenomenon is that, in contrast to the failed unassisted ventricle, the assisted ventricle has stiffer elastic properties and works on the nonlinear portion of diastolic stiffness resulting in increased filling pressures with minimal changes in the LVEDD. Exercise-adjusted pump speeds may still have a beneficial effect on the PV loop morphology as evidenced by return of the PV loop to a more triangular shape when LVAD speed is increased during exercise. At present, unloading provided by Cf-LVADs remains suboptimal.

Ideal algorithms for pump speed during exercise at present are not available, and LV suction remains a pitfall of increasing pump speed.

### Summary

In addition to restoring systemic blood flow and blood pressure, LVADs play a crucial role in unloading the left ventricle and facilitating reverse remodeling and recovery. We have provided an in-depth description of ventricular mechanics, vascular properties, and pump hemodynamics, thus providing a strong foundation for understanding the complex nature of their interactions that determine blood flow to the body, blood pressure, and LV unloading. In practice, these concepts are fundamental to the understanding and interpretation of hemodynamic ramp tests. In addition, we have detailed how factors intrinsic to the pump, the heart, and the vasculature (systemic and pulmonary) impact LVAD-assisted circulation and lead to either suboptimal hemodynamic support or, in extreme



cases, complications such as RV dysfunction and pump thrombosis resulting in hemodynamic collapse.

## References

1. Slaughter MS, Rogers JG, Milano CA, Russell SD, Conte JV, Feldman D, et al. Advanced heart failure treated with continuous-flow left ventricular assist device. *N Engl J Med*. 2009;361(23):2241–51.
2. Miller LW, Pagani FD, Russell SD, John R, Boyle AJ, Aaronson KD, et al. Use of a continuous-flow device in patients awaiting heart transplantation. *N Engl J Med*. 2007;357(9):885–96.
3. Pagani FD, Miller LW, Russell SD, Aaronson KD, John R, Boyle AJ, et al. Extended mechanical circulatory support with a continuous-flow rotary left ventricular assist device. *J Am Coll Cardiol*. 2009;54(4):312–21.
4. Kim G, Uriel N, Burkhoff D. Reverse remodeling and myocardial recovery in heart failure. *Nat Rev Cardiol*. 2018;15(2):83.
5. Hunt SA, Frazier OH. Mechanical circulatory support and cardiac transplantation. *Circulation*. 1998;97(20):2079–90.
6. Moazami N, Fukamachi K, Kobayashi M, Smedira NG, Hoercher KJ, Massiello A, et al. Axial and centrifugal continuous-flow rotary pumps: a translation from pump mechanics to clinical practice. *J Heart Lung Transplant*. 2013;32(1):1–11.
7. Haft J, Armstrong W, Dyke DB, Aaronson KD, Koelling TM, Farrar DJ, et al. Hemodynamic and exercise performance with pulsatile and continuous-flow left ventricular assist devices. *Circulation*. 2007;116(11 Suppl):I8–15.
8. Pagani FD. Continuous-flow rotary left ventricular assist devices with “3rd generation” design. *Semin Thorac Cardiovasc Surg*. 2008;20(3):255–63.
9. Farrar DJ, Bourque K, Dague CP, Cotter CJ, Poirier VL. Design features, developmental status, and experimental results with the Heartmate III centrifugal left ventricular assist system with a magnetically levitated rotor. *ASAIO J*. 2007;53(3):310–5.
10. Capoccia M. Mechanical circulatory support for advanced heart failure: are we about to witness a new “Gold Standard”? *J Cardiovasc Dev Dis*. 2016;3(4):35.
11. Tchoukina I, Smallfield MC, Shah KB. Device management and flow optimization on left ventricular assist device support. *Crit Care Clin*. 2018;34(3):453–63.
12. Griffith BP, Kormos RL, Borovetz HS, Litwak K, Antaki JF, Poirier VL, et al. HeartMate II left ventricular assist system: from concept to first clinical use. *Ann Thorac Surg*. 2001;71(3 Suppl):S116–20; discussion S4–6.
13. Martina J, de Jonge N, Rutten M, Kirkels JH, Kloppe C, Rodermans B, et al. Exercise hemodynamics during extended continuous flow left ventricular assist device support: the response of systemic cardiovascular parameters and pump performance. *Artif Organs*. 2013;37(9):754–62.
14. Potapov EV, Loebe M, Nasser BA, Sinawski H, Koster A, Kuppe H, et al. Pulsatile flow in patients with a novel nonpulsatile implantable ventricular assist device. *Circulation*. 2000;102(19 Suppl 3):III183–7.
15. Tagusari O, Yamazaki K, Litwak P, Antaki JF, Watach M, Gordon LM, et al. Effect of pressure-flow relationship of centrifugal pump on in vivo hemodynamics: a consideration for design. *Artif Organs*. 1998;22(5):399–404.
16. Griffith K, Jenkins E, Pagani FD. First American experience with the Terumo DuraHeart left ventricular assist system. *Perfusion*. 2009;24(2):83–9.
17. Chatterjee K. Coronary hemodynamics in heart failure and effects of therapeutic interventions. *J Card Fail*. 2009;15(2):116–23.
18. Rodbard S, Williams CB, Rodbard D, Berglung E. Myocardial tension and oxygen uptake. *Circ Res*. 1964;14:139–49.
19. Burkhoff D, Sayer G, Doshi D, Uriel N. Hemodynamics of mechanical circulatory support. *J Am Coll Cardiol*. 2015;66(23):2663–74.
20. Burkhoff D, Naidu SS. The science behind percutaneous hemodynamic support: a review and comparison of support strategies. *Catheter Cardiovasc Interv*. 2012;80(5):816–29.
21. Suga H. Total mechanical energy of a ventricle model and cardiac oxygen consumption. *Am J Phys*. 1979;236(3):H498–505.
22. Takaoka H, Takeuchi M, Odake M, Hayashi Y, Hata K, Mori M, et al. Comparison of hemodynamic determinants for myocardial oxygen consumption under different contractile states in human ventricle. *Circulation*. 1993;87(1):59–69.
23. Uriel N, Sayer G, Annamalai S, Kapur NK, Burkhoff D. Mechanical unloading in heart failure. *J Am Coll Cardiol*. 2018;72(5):569–80.
24. Hall JL, Fermin DR, Birks EJ, Barton PJ, Slaughter M, Eckman P, et al. Clinical, molecular, and genomic changes in response to a left ventricular assist device. *J Am Coll Cardiol*. 2011;57(6):641–52.
25. Sunagawa G, Byram N, Karimov JH, Horvath DJ, Moazami N, Starling RC, et al. In vitro hemodynamic characterization of HeartMate II at 6000 rpm: implications for weaning and recovery. *J Thorac Cardiovasc Surg*. 2015;150(2):343–8.
26. Noor MR, Ho CH, Parker KH, Simon AR, Banner NR, Bowles CT. Investigation of the characteristics of HeartWare HVAD and Thoratec HeartMate II under steady and pulsatile flow conditions. *Artif Organs*. 2016;40(6):549–60.
27. Burkhoff D, Dickstein ML, Schleicher T. Harvi – Online. Retrieved from <https://harvi.online/> 2017 updated 4/29/2017. Available from: <http://harvi.online/>.



28. Rich JD, Burkhoff D. HVAD flow waveform morphologies: theoretical foundation and implications for clinical practice. *ASAIO J.* 2017;63(5):526–35.
29. Ayre PJ, Vidakovic SS, Tansley GD, Watterson PA, Lovell NH. Sensorless flow and head estimation in the VentrAssist rotary blood pump. *Artif Organs.* 2000;24(8):585–8.
30. Hornick P, Taylor K. Pulsatile and nonpulsatile perfusion: the continuing controversy. *J Cardiothorac Vasc Anesth.* 1997;11(3):310–5.
31. Russell SD, Rogers JG, Milano CA, Dyke DB, Pagani FD, Aranda JM, et al. Renal and hepatic function improve in advanced heart failure patients during continuous-flow support with the HeartMate II left ventricular assist device. *Circulation.* 2009;120(23):2352–7.
32. Bourque K, Dague C, Farrar D, Harms K, Tamez D, Cohn W, et al. In vivo assessment of a rotary left ventricular assist device-induced artificial pulse in the proximal and distal aorta. *Artif Organs.* 2006;30(8):638–42.
33. Guan Y, Karkhanis T, Wang S, Rider A, Koenig SC, Slaughter MS, et al. Physiologic benefits of pulsatile perfusion during mechanical circulatory support for the treatment of acute and chronic heart failure in adults. *Artif Organs.* 2010;34(7):529–36.
34. Cornwell WK 3rd, Tarumi T, Stickford A, Lawley J, Roberts M, Parker R, et al. Restoration of pulsatile flow reduces sympathetic nerve activity among individuals with continuous-flow left ventricular assist devices. *Circulation.* 2015;132(24):2316–22.
35. Zimpfer D, Strueber M, Aigner P, Schmitto JD, Fiane AE, Larbalestier R, et al. Evaluation of the HeartWare ventricular assist device Lavare cycle in a particle image velocimetry model and in clinical practice. *Eur J Cardiothorac Surg.* 2016;50(5):839–48.
36. Slaughter MS, Pagani FD, Rogers JG, Miller LW, Sun B, Russell SD, et al. Clinical management of continuous-flow left ventricular assist devices in advanced heart failure. *J Heart Lung Transplant.* 2010;29(4 Suppl):S1–39.
37. Uriel N, Sayer G, Addetia K, Fedson S, Kim GH, Rodgers D, et al. Hemodynamic ramp tests in patients with left ventricular assist devices. *JACC Heart Fail.* 2016;4(3):208–17.
38. Uriel N, Morrison KA, Garan AR, Kato TS, Yuzefpolskaya M, Latif F, et al. Development of a novel echocardiography ramp test for speed optimization and diagnosis of device thrombosis in continuous-flow left ventricular assist devices: the Columbia ramp study. *J Am Coll Cardiol.* 2012;60(18):1764–75.
39. Uriel N, Levin AP, Sayer GT, Mody KP, Thomas SS, Adatya S, et al. Left ventricular decompression during speed optimization ramps in patients supported by continuous-flow left ventricular assist devices: device-specific performance characteristics and impact on diagnostic algorithms. *J Card Fail.* 2015;21(10):785–91.
40. Imamura T, Burkhoff D, Rodgers D, Adatya S, Sarswat N, Kim G, et al. Repeated ramp tests on stable LVAD patients reveal patient-specific hemodynamic fingerprint. *ASAIO J.* 2018;64(6):701–7.
41. Grinstein J, Imamura T, Kruse E, Kalantari S, Rodgers D, Adatya S, et al. Echocardiographic predictors of hemodynamics in patients supported with left ventricular assist devices. *J Card Fail.* 2018;24(9):561–7.
42. Pennings KA, Martina JR, Rodermans BF, Lahpor JR, van de Vosse FN, de Mol BA, et al. Pump flow estimation from pressure head and power uptake for the HeartAssist5, HeartMate II, and HeartWare VADs. *ASAIO J.* 2013;59(4):420–6.
43. Klotz S, Deng MC, Stypmann J, Roetker J, Wilhelm MJ, Hammel D, et al. Left ventricular pressure and volume unloading during pulsatile versus nonpulsatile left ventricular assist device support. *Ann Thorac Surg.* 2004;77(1):143–9; discussion 9–50.
44. Garcia S, Kandar F, Boyle A, Colvin-Adams M, Liao K, Joyce L, et al. Effects of pulsatile- and continuous-flow left ventricular assist devices on left ventricular unloading. *J Heart Lung Transplant.* 2008;27(3):261–7.
45. Farrar DJ, Compton PG, Hershon JJ, Fonger JD, Hill JD. Right heart interaction with the mechanically assisted left heart. *World J Surg.* 1985;9(1):89–102.
46. Imamura T, Chung B, Nguyen A, Rodgers D, Sayer G, Adatya S, et al. Decoupling between diastolic pulmonary artery pressure and pulmonary capillary wedge pressure as a prognostic factor after continuous flow ventricular assist device implantation. *Circ Heart Fail.* 2017;10(9):e003882.
47. Nassif ME, Tibrewala A, Raymer DS, Andruska A, Novak E, Vader JM, et al. Systolic blood pressure on discharge after left ventricular assist device insertion is associated with subsequent stroke. *J Heart Lung Transplant.* 2015;34(4):503–8.
48. Patil NP, Mohite PN, Sabashnikov A, Dhar D, Weymann A, Zeriouh M, et al. Does postoperative blood pressure influence development of aortic regurgitation following continuous-flow left ventricular assist device implantation? *Eur J Cardiothorac Surg.* 2016;49(3):788–94.
49. Najjar SS, Slaughter MS, Pagani FD, Starling RC, McGee EC, Eckman P, et al. An analysis of pump thrombus events in patients in the HeartWare ADVANCE bridge to transplant and continued access protocol trial. *J Heart Lung Transplant.* 2014;33(1):23–34.
50. Akimoto T, Yamazaki K, Litwak P, Litwak KN, Tagusari O, Mori T, et al. Relationship of blood pressure and pump flow in an implantable centrifugal blood pump during hypertension. *ASAIO J.* 2000;46(5):596–9.
51. Fagard R. Athlete's heart. *Circulation.* 2001;103(6):E28–9.
52. Fresiello L, Rademakers F, Claus P, Ferrari G, Di Molfetta A, Meyns B. Exercise physiology with a left ventricular assist device: analysis of heart-pump interaction with a computational simulator. *PLoS One.* 2017;12(7):e0181879.



53. Loyaga-Rendon RY, Plaisance EP, Arena R, Shah K. Exercise physiology, testing, and training in patients supported by a left ventricular assist device. *J Heart Lung Transplant*. 2015;34(8):1005–16.
54. Hayward CS, Fresiello L, Meyns B. Exercise physiology in chronic mechanical circulatory support patients: vascular function and beyond. *Curr Opin Cardiol*. 2016;31(3):292–8.
55. Pina IL, Apstein CS, Balady GJ, Belardinelli R, Chaitman BR, Duscha BD, et al. Exercise and heart failure: a statement from the American Heart Association Committee on exercise, rehabilitation, and prevention. *Circulation*. 2003;107(8):1210–25.
56. Akimoto T, Yamazaki K, Litwak P, Litwak KN, Tagusari O, Mori T, et al. Rotary blood pump flow spontaneously increases during exercise under constant pump speed: results of a chronic study. *Artif Organs*. 1999;23(8):797–801.
57. Muthiah K, Gupta S, Otton J, Robson D, Walker R, Tay A, et al. Body position and activity, but not heart rate, affect pump flows in patients with continuous-flow left ventricular assist devices. *JACC Heart Fail*. 2014;2(4):323–30.
58. Hu SX, Keogh AM, Macdonald PS, Kotlyar E, Robson D, Harkess M, et al. Interaction between physical activity and continuous-flow left ventricular assist device function in outpatients. *J Card Fail*. 2013;19(3):169–75.
59. Jacquet L, Vancaenegem O, Pasquet A, Matte P, Poncelet A, Price J, et al. Exercise capacity in patients supported with rotary blood pumps is improved by a spontaneous increase of pump flow at constant pump speed and by a rise in native cardiac output. *Artif Organs*. 2011;35(7):682–90.
60. Schima H, Vollkron M, Jantsch U, Crevenna R, Roethy W, Benkowski R, et al. First clinical experience with an automatic control system for rotary blood pumps during ergometry and right-heart catheterization. *J Heart Lung Transplant*. 2006;25(2):167–73.
61. Brassard P, Jensen AS, Nordsborg N, Gustafsson F, Moller JE, Hassager C, et al. Central and peripheral blood flow during exercise with a continuous-flow left ventricular assist device: constant versus increasing pump speed: a pilot study. *Circ Heart Fail*. 2011;4(5):554–60.
62. Muthiah K, Robson D, Prichard R, Walker R, Gupta S, Keogh AM, et al. Effect of exercise and pump speed modulation on invasive hemodynamics in patients with centrifugal continuous-flow left ventricular assist devices. *J Heart Lung Transplant*. 2015;34(4):522–9.
63. Burkhoff D, Dickstein ML, Schleicher T. Harvi – Online. Retrieved from <http://harvi.online/>. 2017.